

Efficient Vision-and-Language Pre-training with Text-Relevant Image Patch Selection

Wei Ye^{1†}, Chaoya Jiang^{1†}, Haiyang Xu^{2*}, Qinghao Ye², Chenliang Li²,
Ming Yan², Shikun Zhang^{1*}, Songfang Huang², Fei Huang²

^{1*}National Engineering Research Center for Software Engineering, Peking University,
Beijing, China.

²DAMO Academy, Alibaba Group, Beijing, China.

*Corresponding author(s). E-mail(s): shuofeng.xhy@alibaba-inc.com;
zhangsk@pku.edu.cn;

Contributing authors: weiy@pku.edu.cn; jiangchaoya@pku.edu.cn;
yeqinghao.yqh@alibaba-inc.com; lcl193798@alibaba-inc.com; ym119608@alibaba-inc.com;
songfang.hsf@alibaba-inc.com; fei.huang@alibaba-inc.com;

[†]These authors contributed equally to this work.

Abstract

Vision Transformers (ViTs) have become increasingly popular in large-scale Vision and Language Pre-training (VLP) models. Although previous VLP research has demonstrated the efficacy of ViTs, these efforts still struggle with computational inefficiencies caused by lengthy visual sequences. To address this challenge, we introduce an efficient VLP approach called TRIPS, which stands for **Text-Relevant Image Patch Selection**. TRIPS progressively reduces the visual sequence using a text-guided patch-selection layer in the visual backbone, thereby accelerating both training and inference processes. This patch-selection layer dynamically computes text-dependent visual attention, enabling it to identify attentive image tokens with text guidance and fuse inattentive ones in an end-to-end fashion. Importantly, TRIPS does not add any extra parameters and generalizes to most ViT-based VLP models. We incorporate TRIPS into three representative VLP models covering single-stream, dual-stream, and generative paradigms, and conduct extensive experiments on five widely-used multi-modal benchmark datasets. Our experimental results reveal that TRIPS delivers a 40% speedup, while maintaining competitive or superior performance on downstream tasks.

Keywords: Vision-Language pre-training, Patch Selection, Efficiency

1 Introduction

In recent years, Vision-Language Pre-training (VLP) (Tan and Bansal, 2019; Chen et al, 2019; Lu et al, 2019; Huang et al, 2020; Li et al, 2020; Chen et al, 2020; Zhou et al, 2020; Li et al,

2021; Yu et al, 2021) has experienced remarkable growth, emerging as a dominant paradigm for addressing Vision-Language (VL) tasks. Conventional VLP models (Tan and Bansal, 2019; Chen et al, 2019; Lu et al, 2019; Li et al, 2020) employ pre-trained object detectors (Ren et al, 2015; Redmon et al, 2016; He et al, 2017) to

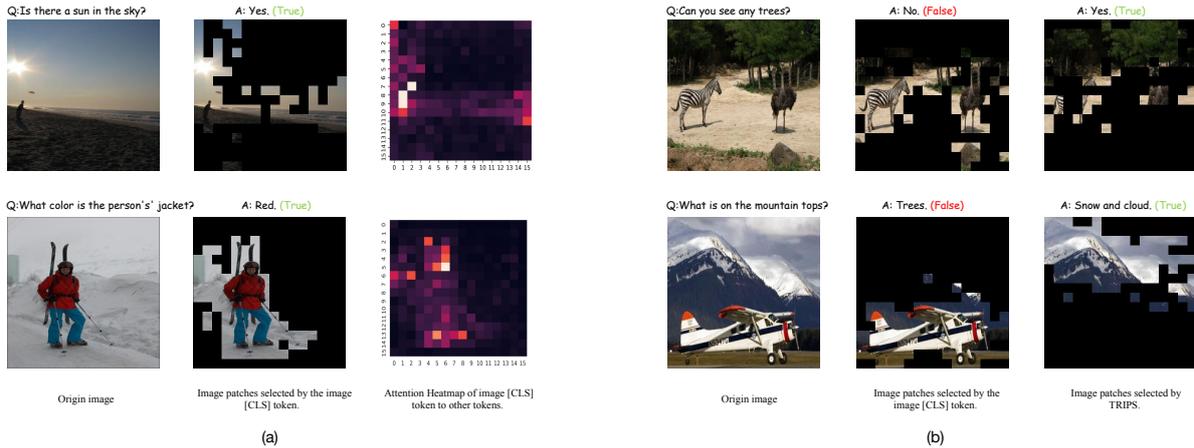


Fig. 1 Sub-figure (a) presents the VQA cases for ALBEF (Li et al, 2021) fine-tuned on the VQA task, where input image tokens are directly selected based on the attention weight of the image [CLS] token in relation to other image tokens. We visualize the attention distribution of the image [CLS] token, which, as seen, naturally concentrates on objects within the images while disregarding the backgrounds. If the question pertains to the objects in the images, accurate predictions can be obtained. Sub-figure (b) compares VQA predictions between ALBEF, which directly selects image tokens guided by the image [CLS] token, and our model, TRIPS-ALBEF. As illustrated, when questions relate to image backgrounds, the former produces incorrect answers, whereas the latter provides the right responses by preserving text-relevant image tokens.

extract region-based image features but suffer from extensive annotation and expensive computation of object detector training. Inspired by the success of the Vision Transformer (ViT) (Dosovitskiy et al, 2021) and its variants (Liu et al, 2021; Wu et al, 2021; Wang et al, 2021b) in the computer vision domain, more recent VLP models (Li et al, 2021; Radford et al, 2021; Kim et al, 2021; Wang et al, 2021a; Singh et al, 2021) have adopted ViT as the visual encoder or cross-modal fusion encoder without using region features from the pre-trained object detector.

However, ViT-based VLP methods necessitate the modeling of lengthy visual sequences, e.g., from high-resolution images, to achieve robust vision understanding, which results in quadratic computational complexity proportional to the visual sequence length. Furthermore, recent studies (Dosovitskiy et al, 2021; Touvron et al, 2021) have started to investigate vision-language foundation models, focusing on scaling up both model and data size. Consequently, there is an increasing need to reduce the substantial computational costs associated with ViT-based VLP models. As demonstrated in Figure 1 (a), we observe that eliminating the inattentive patch tokens of the image [CLS] token generally does not impact the Visual Question Answering (VQA) (Agrawal et al, 2015) predictions. Based on this observation, we hypothesize that not all image tokens in the visual

encoder positively contribute to the final prediction results of VLP models, and a considerable number of redundant image tokens exist.

Recent studies (Rao et al, 2021; Xu et al, 2021b; Zong et al, 2021; Liang et al, 2022) have explored ViT model acceleration by eliminating unrelated image tokens. However, these methods are specifically tailored for computer vision tasks (e.g., image recognition) and remove redundant tokens based on visual semantics while disregarding the aligned knowledge in the text modality. Consequently, they are not suitable for VL tasks. As illustrated in Figure 1 (b), removing patch tokens based solely on the image [CLS] token, without the guidance of text knowledge, leads to incorrect answers. This observation inspires us to reduce the number of image tokens by merging less informative patch tokens under the guidance of the aligned text context.

In this work, we introduce an efficient VLP model featuring Text-Relevant Image Patch Selection (TRIPS) to progressively reduce redundant image tokens with the guidance of text. TRIPS selects text-consistent image tokens through a text-aware patch-selection layer, thereby minimizing the computational cost of visual encoding and cross-modal fusion. This patch-selection layer preserves attentive image tokens with text guidance and fuses inattentive tokens into a single one by dynamically computing text-dependent visual

attention in an end-to-end manner. Consequently, we gradually decrease the number of image tokens as the visual backbone deepens, alleviating the computational burden of the visual encoder and enhancing the efficiency of cross-modal fusion due to the reduced visual sequences. Additionally, model efficiency can be flexibly controlled by adjusting the keep rate of image tokens in the patch-selection layer without introducing any additional parameters.

We evaluate TRIPS on five representative VL tasks consisting of visual question answering (VQA), natural language visual reasoning (NLVR), cross-modal retrieval, image captioning, and visual grounding. By incorporating TRIPS into existing representative VLP models, we achieve approximately 40% efficiency gains while maintaining competitive or superior downstream task performance. For example, equipped with TRIPS, ALBEF (Li et al, 2021), a recent robust two-stream VLP model, can accelerate by 40.98% and even improve by 0.1 on the VQA test-dev and 0.2 on the NLVR Dev (see Table 3). Moreover, by increasing the input image resolution while maintaining the same computational cost, TRIPS can enhance performance by 0.4 on the VQA test-dev and 0.6 on the NLVR Dev.

Our main contributions can be summarized as three-fold:

- We introduce an efficient vision-and-language pre-training model featuring Text-Relevant Image Patch Selection (TRIPS). To the best of our knowledge, this is the first attempt to reduce the computational cost of VLP models by diminishing image tokens with the assistance of linguistic context.
- We propose a novel text-relevant patch-selection layer, which can dynamically compute text-dependent visual attention to identify attentive (or critical) image tokens and merge inattentive ones with text guidance in an end-to-end manner.
- Comprehensive experiments demonstrate that our TRIPS can enhance the training and inference efficiency of VLP models while incurring lower computational costs. Moreover, by increasing the input image resolution, TRIPS leverages additional image tokens to achieve superior performance without increasing computational expenses.

2 Related Work

2.1 Vision-Language Pre-training

Current approaches to VLP can be broadly divided into two categories in terms of visual representation extraction. The first category is detector-based VLP methods (Lu et al, 2019; Li et al, 2019; Tan and Bansal, 2019; Li et al, 2020; Chen et al, 2020; Yu et al, 2021). These methods primarily adopt a two-step training pipeline: they extract visual features using a pre-trained object detector and then train the cross-modal pre-training model to align text and visual features. Some region-based methods aim to reduce computational costs with lightweight model architectures (Wang et al, 2020a; Gan et al, 2021) or knowledge distillation (Fang et al, 2021). However, these methods still face several challenges, including expensive computation and time consumption for object/region detection and error propagation problems caused by the two-step pre-training strategy. The main challenge for these methods is to balance effectiveness and efficiency. The second category consists of more recent CNN-based (Huang et al, 2020; Xu et al, 2021a) or ViTs-based (Li et al, 2021; Kim et al, 2021; Radford et al, 2021; Wang et al, 2021a) methods, especially patch-based ViT. These methods eliminate the need for a complex object detector in feature extraction, enabling end-to-end VL learning. However, few works have focused on reducing the high computational cost of ViT-based VLP models.

In terms of fusion schemes for modeling cross-modal interaction, typical VLP approaches (Tan and Bansal, 2019; Li et al, 2021, 2020; Wang et al, 2021c; Kim et al, 2021; Li et al, 2022b; Wang et al, 2021a) can also be categorized into *dual stream* and *single stream*. Single-stream approaches (Li et al, 2020; Kim et al, 2021; Wang et al, 2021c,a) assume that the potential correlation and alignment between the two modalities are relatively straightforward and can be learned by a single transformer encoder. As a result, the architecture concatenates text embeddings and image features, along with special embeddings that indicate their respective positions and modalities. This concatenated feature set is then fed into a transformer-based encoder for further processing. Dual-stream approaches (Tan and Bansal, 2019; Li et al, 2022a,b; Dou et al, 2021; Xu

et al, 2021a) assume that the intra-modal interaction and cross-modal interaction need to be separated to obtain better multimodal representations. Thus, they employ two single-modal encoders to separately encode images and text. Additionally, previous VLP methods (Li et al, 2019; Chen et al, 2019; Su et al, 2020; Wang et al, 2021a) were typically only capable of performing tasks related to vision-language understanding and reasoning (e.g., VQA and NLVR). However, recent multimodal generation models (Li et al, 2022b,a; Wang et al, 2021c) have started to adopt encoder-decoder style generative approaches for accomplishing tasks associated with multimodal text generation. Our method can easily generalize to most ViT-based VLP models, including single-stream, dual-stream, and generative approaches.

2.2 ViTs Acceleration

Numerous studies have focused on proposing more efficient attention mechanisms (Wang et al, 2020b; Kitaev et al, 2020; Choromanski et al, 2021) or compressing Transformer structures (Liu et al, 2021; Heo et al, 2021; Wang et al, 2021b) to accelerate the computation of transformer-based models (Vaswani et al, 2017). Recently, some approaches have aimed to accelerate ViTs by reducing the number of tokens involved in ViT inference. For instance, (Ryoo et al, 2021) proposed TokenLearner to expedite ViTs, in which a relatively small number of tokens are learned by aggregating the entire feature map weighted by dynamic attention. (Rao et al, 2021) introduces a method to reduce tokens for a fully trained ViT, where an extra learnable neural network is added to ViT to select a subset of tokens. (Liang et al, 2022) proposes to reduce the computational overhead of inference by introducing a token reorganization method to progressively reduce and reorganize image tokens. However, these methods are not suitable for VLP, as they reduce image tokens without considering the text context. In contrast, our proposed approach takes into account the textual context, making it more appropriate for VLP tasks.

3 Method

Our method aims to generalize to most ViT-based VLP models covering single-stream, dual-stream,

and generative VLP paradigms. In this section, we mainly use the dual-stream ALBEF (Li et al, 2021) framework as a representative base model to introduce the technical design of our TRIPS (named TRIPS-ALBEF). We will first present the model architecture, and then introduce the ViT-based visual backbone with the acceleration module of the text-relevant patch-selection layer. We will also briefly discuss how we incorporate TRIPS into a recent generative VLP model mPLUG (Li et al, 2022a) and single-stream model ViLT (Kim et al, 2021). Finally, we will introduce the pre-training objectives.

3.1 Model Architecture

As shown in Figure 2 (a), TRIPS-ALBEF contains a visual encoder with the text-relevant patch-selection layer, a text encoder, and a multimodal fusion encoder. The visual encoder takes a Vision Transformer (ViT), where text-relevant patch-selection layers are used to progressively reduce and reorganize image tokens, namely ViT-TRIPS. The text encoder adopts BERT_{base} transformer (Devlin et al, 2019). Similar to Li et al (2021), the multimodal fusion encoder is a transformer encoder that performs the cross-modal interaction and fusion through a cross-attention mechanism.

Formally, given an input image-text pair, we first feed the input text to the text encoder and represent it as a sequence of embeddings $T = \{t_{cls}, t_1, t_2, \dots, t_m\}$, where t_{cls} is the embedding of the text [CLS] token to summarize the input text. Then, we divide the input image into patches $P = \{p_{cls}, p_1, p_2, \dots, p_u\}$, and encode them with the image encoder ViT-TRIPS. It takes the text [CLS] embedding t_{cls} and image patches $\{p_{cls}, p_1, p_2, \dots, p_u\}$ as input, and outputs the image sequence $V = \{v_{cls}, v_1, v_2, \dots, v_e\}$. Note that $e < u$, since we apply the text-relevant patch-selection layer to select the text-aware image tokens and fuse the redundant tokens, allowing us to reduce the total visual sequence length for efficiency. Finally, the text features $\{t_{cls}, t_1, t_2, \dots, t_m\}$ and the image features $\{v_{cls}, v_1, v_2, \dots, v_e\}$ encoded by the image encoder are fused by cross attention at each layer of the multimodal encoder as in ALBEF (Li et al, 2021). The output of the multimodal encoder is used to pre-train and finetune downstream tasks.

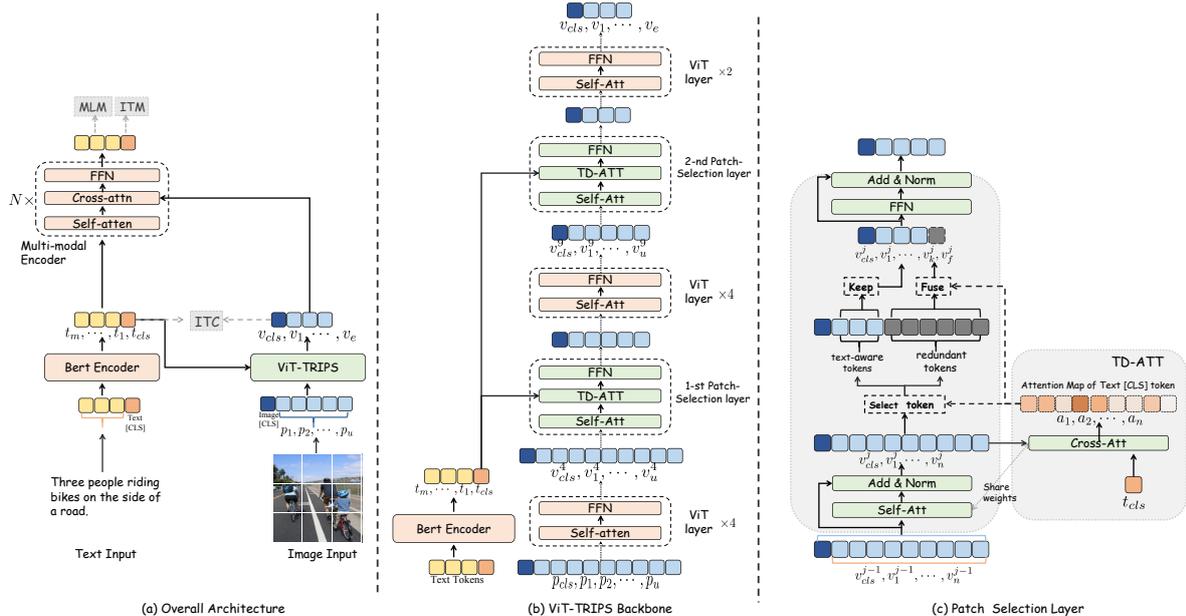


Fig. 2 Sub-figure (a) showcases the overall architecture of the VLP model (TRIPS-ALBEF) presented in this paper. Sub-figure (b) provides a visual overview of the ViT augmented with a Text-Relevant Image Patch Selection module (ViT-TRIPS). We assume the ViT-TRIPS comprises 12 layers, and the 5th and 10th layers serve as the patch selection layers. Sub-figure (c) depicts the design of the Text-Relevant Image Patch Selection layer.

3.2 Text-Relevant Image Patch Selection

Existing works in computer vision (Rao et al, 2021; Liang et al, 2022) select patches by using only the image [CLS] token from the ViT backbone. However, as shown in Figure 1 (b), the selection of image tokens in cross-modal tasks is closely related to textual context, and different texts for a single image may focus on different parts of the visual content. Selecting the image tokens with the guidance of aligned textual content can help the VLP model focus on the key parts of the image for more effective and efficient cross-modal fusion. Here, we present a text-relevant patch-selection layer that can dynamically select the image patches with the guidance of textual input, yet with no additional parameters introduced.

As shown in Figure 2 (b), for a ViT with L standard Transformer layers and t patch-selection layers in total, the interval length is obtained as $s = L/(t + 1)$. Then, we choose the layer index $j = i * s + 1$ as the i_{th} patch-selection layer, so that patch-selection layers are uniformly inserted into the ViT-TRIPS backbone. In each patch-selection layer, as shown in Figure 2(c), we adopt standard self-attention (SA), Text-aware

Dynamic Attention (TD-ATT), and Inattentive Token Fusion (ITF) modules to progressively reduce image tokens.

Specifically, for the i_{th} patch-selection layer, image features $v^{j-1} = \{v_{cls}^{j-1}, v_1^{j-1}, \dots, v_n^{j-1}\}$ are first fed to the j_{th} visual self-attention layer:

$$v^j = LN(SA(v^{j-1}) + v^{j-1}) \quad (1)$$

where LN is short for layer normalization, and n is the number of patch tokens in the $j - 1$ visual transformer layer. Next, we will illustrate how to use the Text-aware Dynamic Attention mechanism (TD-ATT) to select the text-aware image patch tokens. The text [CLS] embedding t_{cls} is linearly projected to the query vector denoted as q_{text} by the shared query linear layer of the j_{th} visual self-attention layer. We compute the text-to-image attention feature map excluding the image [CLS] token as follows:

$$a_{cls} = softmax\left(\frac{q_{text} \cdot v^j[1:]^T}{\sqrt{d}}\right) \quad (2)$$

We identify and preserve the attentive image tokens corresponding to the k largest elements in the attention map $a_{cls} = \{a_1, \dots, a_n\}$, where $k = n \times r$, and r is the keep rate of this layer. The selected

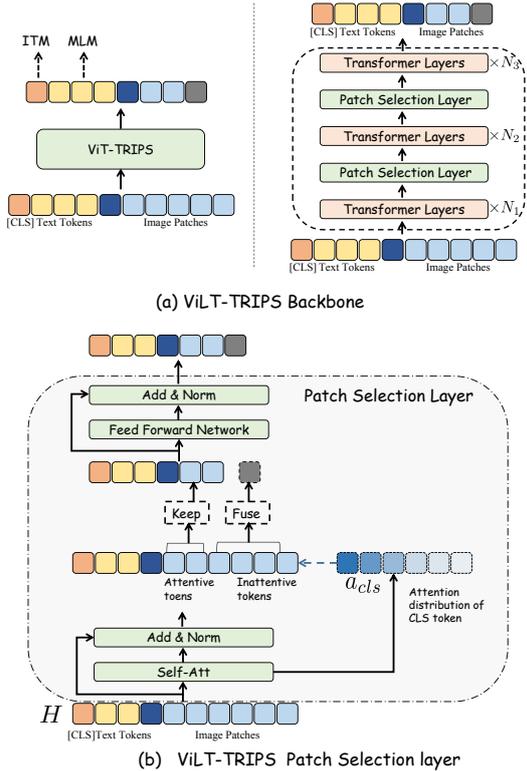


Fig. 3 Sub-figure (a) depicts the ViT-TRIPS backbone of the single-stream VLP model. Sub-figure (b) is the illustration of the Text-Relevant Image Patch-Selection layer.

image tokens are kept, and the un-selected image tokens are further fused by an inattentive token fusion operation ITF.

The remaining inattentive patch tokens $\{v_{z_1}, v_{z_2}, \dots, v_{z_{n-k}}\}$ are treated as text-irrelevant tokens. However, the fixed keep rate may remove some useful tokens, so we fuse inattentive tokens to one token v_f by a weighted sum operation to supplement attentive ones as follow:

$$v_f = \sum_{i=1}^{n-k} a_{cls, z_i} \cdot \hat{v}_{z_i} \quad (3)$$

After fusing the inattentive patch tokens, we reconstruct the j_{th} visual sequence as $v^j = [v_{cls}^j, v_1^j, \dots, v_k^j, v_f^j]$, which consists of the image [CLS] token embedding, the selected text-aware image patch embedding, and fused inattentive patch embedding. Then the new visual sequence is fed to the feed-forward network (FFN).

3.3 Extension to Generative VLP Models

Our method can be easily applied to generative vision-language models. We extend TRIPS to the latest state-of-the-art dual-stream generative model mPLUG (Li et al, 2022a), referred to as TRIPS-mPLUG. Specifically, we replace the ViT-based visual backbone in mPLUG with ViT-TRIPS while keeping other settings unchanged.

3.4 Extension to Single-stream VLP Models

The proposed Text-Relevant Image Patch Selection layer can also be extended to single-stream models, which employ the [CLS] token of the multimodal encoder to preserve attentive image tokens and fuse inattentive tokens to accelerate training and inference. In this paper, we implement this model, denoted as TRIPS-ViLT, based on the ViLT (Kim et al, 2021) framework, a widely used single-stream model. As shown in Figure 3, the single-stream model has a global [CLS] token for aggregating visual and linguistic information, allowing us to directly select text-aware visual tokens and fuse unrelated image patch tokens based on the attention weights of the [CLS] tokens to image patch tokens.

3.5 Pre-training Objectives

Table 1 Pre-training tasks of different TRIPS variants.

Model	ITC	ITM	MLM	PrefixLM
TRIPS-ViLT	✗	✓	✓	✗
TRIPS-ALBEF	✓	✓	✓	✗
TRIPS-mPLUG	✓	✓	✓	✓

We pre-train our models with the following standard objectives: Image-Text Contrastive learning (ITC), Image-Text Matching (ITM), and Masked Language Modeling (MLM). These pre-training tasks are optimized jointly. As shown in Table 1, the three TRIPS variants differ in the combination of pre-training tasks.

Image-Text Contrastive (ITC) For TRIPS-ALBEF and TRIPS-mPLUG, we follow (Li et al, 2021) and apply ITC to align the image representation and text representation from the unimodal encoders.

Image-Text Matching (ITM) The goal of image-text matching is to predict whether the input image and text are matched, which is a shared task among all model variants. We follow the design of (Li et al, 2021) and select hard negative image-text pairs based on the contrastive text-image similarity. We take the text [CLS] embedding of the multimodal encoder’s output as the joint representation, followed by a Multi-Layer Perceptron (MLP) layer for prediction.

Masked Language Modeling (MLM) The task setup is essentially the same as in BERT (Devlin et al, 2019), where we randomly mask 15% of tokens in text and the model is asked to predict these masked words with the cross-modal representations.

Prefix Language Modeling (PrefixLM). This task is specific to mPLUG (Li et al, 2022a), which aims to generate a caption given an image and predict the text segment subsequent to the cross-modal context as in (Bi et al, 2020). It optimizes a cross-entropy loss by maximizing the likelihood of text in an autoregressive manner.

4 Experiment Settings

4.1 Implementation Details

We pre-train TRIPS-ALBEF and TRIPS-mPLUG for 30 epochs, and TRIPS-ViT for 20 epochs with a total batch size of 512 on 8 NVIDIA V100 GPUs. We initialize the visual encoder using CLIP (ViT-B/16) (Radford et al, 2021) pre-trained on 400M noisy image-text pairs and employ the AdamW (Loshchilov and Hutter, 2019) optimizer with a weight decay of 1e-2. The learning rate is warmed up to 1e-5 (ViT-B/16) and 1e-4 (BERT_{base}) in the first 1000 iterations. During pre-training, we use input images with a resolution of 256×256 and increase the image resolution during fine-tuning. For TRIPS-ALBEF and TRIPS-mPLUG, we utilize a 6-layer Transformer for both the text encoder and the cross-modal fusion network. Following Li et al (2021), we initialize the text encoder with the first 6 layers of BERT_{base} (Devlin et al, 2019) and the cross-modal network with the last 6 layers of BERT_{base}. For image-text contrastive learning, we set the queue size to 65,536 and the momentum coefficient to 0.995.

In the proposed TRIPS-ViT backbone, we designate the 5th and 10th layers as patch-selection layers and set the keep rate for each layer to 70%, achieving a balance between downstream task performance and model inference speed. Details of fine-tuning hyperparameters can be found in Appendix B.

We use the AdamW optimizer (Loshchilov and Hutter, 2019) with a weight decay of 0.02 to train our models. For TRIPS-ALBEF and TRIPS-mPLUG, we warm up the learning rate to 1e-5 (ViT-B/16) and 1e-4 (BERT_{base}) in the first 1000 iterations, then decay it to 1e-6 according to a cosine schedule. Pre-training TRIPS-ALBEF takes approximately 60 hours, TRIPS-mPLUG takes around 80 hours, and TRIPS-ViT requires about 40 hours; all performed on 8 V100-32G GPUs using a 4M pre-training dataset for approximately 20 epochs.

To enhance the generalization of vision encoders during pre-training, we apply RandAugment (Cubuk et al, 2020) to random image crops of size 256 × 256. In the fine-tuning stage for VQA, image captioning, and visual grounding tasks, we increase the image resolution. For image-text contrastive learning, we set the queue size to 65,536 and the momentum coefficient to 0.995.

4.2 pre-training data

Table 2 Statistics of the pre-training datasets.

	COCO	VG	SBU	CC3M
image	113K	100K	860K	3M
text	567K	769K	860K	3M

We construct our pre-training data using two web datasets (Conceptual Captions (Sharma et al, 2018), SBU Captions (Ordonez et al, 2011)) and two in-domain datasets (MSCOCO (Lin et al, 2014) and Visual Genome (Krishna et al, 2016)). The total number of unique images is 4.0M, and the number of image-text pairs is 5.1M. Table 2 shows the statistics of the 4M images with texts used in the pre-training stage.

5 Experiment Results

5.1 Overall Performance

We evaluate TRIPS-ALBEF, TRIPS-mPLUG, and TRIPS-ViLT on five vision-language downstream tasks: visual question answering (VQA), natural language for visual reasoning (NLVR), image-text retrieval, image captioning, and visual grounding. Our baselines cover 15 VLP models, which is detailed in Section A. We will first analyze their overall performances on these tasks.

5.1.1 Visual Question Answering

The VQA task (Agrawal et al, 2015) requires the model to answer natural language questions given an image. Following (Li et al, 2021), we treat VQA as an answer generation problem. We report test-dev and test-std scores by submitting our results to the evaluation server¹, as shown in Table 3. Looking into Table 3, VLP models equipped with ViT-TRIPS improve performance on the VQA task (e.g., ViLT (Kim et al, 2021) achieves 71.26 on Test-dev, while TRIPS-ViLT scores 71.48; ALBEF (Li et al, 2021) reaches 76.12, while TRIPS-ALBEF attains 76.23). These results are impressive, considering they are achieved with significantly reduced training and inference costs (see more details of efficiency in Section 5.2).

5.1.2 Natural Language for Visual Reasoning

The NLVR2 (Suhr et al, 2019) task requires the model to predict whether a sentence accurately describes a pair of images, which is a binary classification task. For TRIPS-ALBEF and TRIPS-mPLUG, we follow (Li et al, 2021) and use two cross-attention layers to process the two input images; their outputs are merged and fed into a Feed Forward Network (FFN). An MLP classifier is then applied to the output embedding of the text [CLS] token. For TRIPS-ViLT, we follow (Kim et al, 2021) and use the pairing method. The input is reformulated into two pairs (question, image1) and (question, image2), and each pair goes through TRIPS-ViLT. The classification head takes the concatenation of two

Table 3 Evaluation Results on VQA and NLVR². More details about comparison models are in Appendix A.

model	# Pre-train Data	VQA		NLVR2	
		Test-dev	Test-std	Dev	Test-P
E2E-VLP	4M	73.25	73.67	77.25	77.96
OSCAR _{Base}	6.5M	73.16	73.44	78.07	78.36
VinVL _{Large}	5.65M	76.52	76.60	82.67	83.98
ViLBERT	3.3M	70.63	70.92	-	-
VisualBERT	180K	70.80	71.00	67.40	67.00
LXMERT	180K	72.42	72.54	74.90	74.50
UNITER _{Large}	4M	73.82	74.02	79.12	79.98
METER _{CLIP}	4M	77.68	77.64	82.33	83.05
BLIP _{Base}	14M	77.54	77.62	82.67	82.30
VLMo _{Large}	4M	76.64	76.89	82.77	83.34
SimVLM _{Base}	1.8B	77.87	78.14	81.72	81.77
ViLT _{Base}	4M	71.26	71.29	75.18	76.2
TRIPS-ViLT	4M	71.48	71.52	75.89	76.4
ALBEF _{Base}	4M	76.12	76.32	82.21	83.1
TRIPS-ALBEF	4M	76.23	76.48	82.35	83.34
mPLUGG _{Base}	4M	77.80	77.98	83.76	83.92
TRIPS-mPLUG	4M	77.89	78.23	83.87	84.04

pooled representations as input and outputs the binary prediction. As shown in Table 3, TRIPS outperforms existing VLP methods.

5.1.3 Image-Text Retrieval

We conduct experiments for both image-to-text retrieval (TR) and text-to-image retrieval (IR) on MSCOCO (Lin et al, 2014) and Flickr30K (Plummer et al, 2015) datasets. We jointly optimize the ITC loss and the ITM loss during fine-tuning. Results are reported in Table 4. As illustrated in Table 4, our model achieves comparable performance to other VLP baselines.

5.1.4 Image Captioning

To investigate the text generation capacity of TRIPS-mPLUG, we evaluate it on the image captioning task. Since there is no textual input for this task, we select visual semantic-aware patches based on the attention weight of the image [CLS] token to other image tokens and fuse other image tokens based on the attention weight. We perform this operation based on the observation that the image [CLS] token in ViTs pays more attention (i.e., having a larger attention value) to class-specific tokens than to tokens on non-object regions (Caron et al, 2021). Following Li et al (2020), we fine-tune TRIPS-mPLUG with cross-entropy loss and then with CIDEr optimization for an additional 5 epochs. Our experiments, as shown

¹<https://eval.ai/web/challenges/challenge-page/830/overview>

Table 4 Evaluation results of image-text retrieval on Flickr30K (Plummer et al, 2015) and COCO datasets (Lin et al, 2014).

Models	# Pre-train data	MSCOCO (5K test set)						Flickr30K (1K test set)					
		TR			IR			TR			IR		
		R@1	R@5	R@10	R@1	R@5	R@10	R@1	R@5	R@10	R@1	R@5	R@10
E2E-VLP	4M	-	-	-	-	-	-	86.2	97.5	98.92	73.6	92.4	96.0
OSCAR _{Base}	4M	70.0	91.1	95.5	54.0	80.8	88.5	-	-	-	-	-	-
VinVL _{Large}	5.65M	75.4	92.9	96.2	58.8	83.5	90.3	-	-	-	-	-	-
ViLBert	3.3M	-	-	-	-	-	-s	-	-	-	58.2	84.9	91.5
UNITER _{Large}	4M	65.7	88.6	93.8	52.9	79.9	88.0	87.3	98.0	99.2	75.6	94.1	96.8
METER _{CLIP}	4M	76.2	93.2	96.8	57.1	82.7	90.1	94.3	99.6	99.9	82.2	96.3	98.4
VLMo _{Large}	4M	78.2	94.4	97.4	60.6	84.4	91.0	95.3	99.9	100.0	84.5	97.3	98.6
BLIP _{Base}	14M	80.6	95.2	97.6	63.1	85.3	91.1	96.6	99.8	100.0	87.2	97.5	98.8
ViLT	4M	61.5	86.3	92.7	42.7	72.9	83.1	83.5	96.7	98.6	64.4	88.7	93.8
TRIPS-ViLT	4M	63.2	88.2	94.1	43.9	74.1	84.6	85.4	98.3	98.4	64.4	89.2	94.9
ALBEF _{Base}	4M	77.8	94.3	97.4	60.3	84.7	91.0	95.9	99.8	100.0	85.6	97.5	98.9
TRIPS-ALBEF	4M	78.1	94.8	97.6	61.3	84.3	91.4	96.3	99.8	100.0	85.8	98.1	99.0
mPLUG _{Base}	4M	80.5	95.4	97.9	63.3	85.3	91.2	96.7	99.8	100.0	86.5	97.5	98.9
TRIPS-mPLUG	4M	80.8	95.7	98.0	63.6	85.5	91.5	97.0	99.8	100.0	86.9	97.8	99.1

Table 5 Evaluation Results on image captioning on COCO Karpathy test split (Karpathy and Fei-Fei, 2015). B@4: BLEU@4, M: METEOR, C: CIDEr, S: SPICE.

Models	# Pre-train Data	COCO Caption							
		Cross-entropy Optimization				CIDEr Optimization			
		B@4	M	C	S	B@4	M	C	S
E2E-VLP	4M	36.2	-	117.3	-	-	-	-	-
OSCAR _{Base}	6.5M	36.5	30.3	123.7	23.1	40.5	29.7	137.6	22.8
VinVL _{Large}	5.65M	38.5	30.4	130.8	23.4	41.0	31.1	140.9	25.2
BLIP _{Base}	14M	38.6	-	129.7	-	-	-	-	-
SimVLM _{Base}	1.8B	39.0	32.9	134.8	24.0	-	-	-	-
mPLUG _{Base}	4M	39.3	30.1	132.4	23.34	41.2	31.0	140.8	25.2
TRIPS-mPLUG	4M	39.4	30.5	132.8	23.82	41.5	30.9	141.2	25.4

in Table 5, demonstrate that TRIPS-mPLUG achieves comparable results with state-of-the-art models.

5.1.5 Visual Grounding

Following the setting of mPLUG (Li et al, 2022a), we also evaluate TRIPS-mPLUG on the visual grounding task, which requires models to localize the referred object in the image based on a given text query. Instead of directly regressing the bounding boxes, we concatenate visual features and attended textual features and feed them into the decoder to predict the coordinates. Table 6 demonstrates the performance of TRIPS-mPLUG in the visual grounding task.

Table 6 Evaluation results of visual grounding on ReferCOCO+. We use the accuracy of IOU 0.5 on visual grounding (a prediction is right if the IoU between the grounding-truth box and the predicted bounding box is larger than 0.5)

Model	RefCOCO+		
	testA	testB	val
UNITER _{Large}	75.90	81.45	66.70
ViLBERT	72.34	78.52	62.61
VILLA	76.17	81.54	66.84
MDETR	79.52	84.09	70.62
UNICORN	80.30	85.05	71.88
mPLUG _{Base}	80.07	85.21	71.03
TRIPS-mPLUG	80.11	86.03	71.21

TRIPS-mPLUG achieves comparable results with competitive baseline methods.

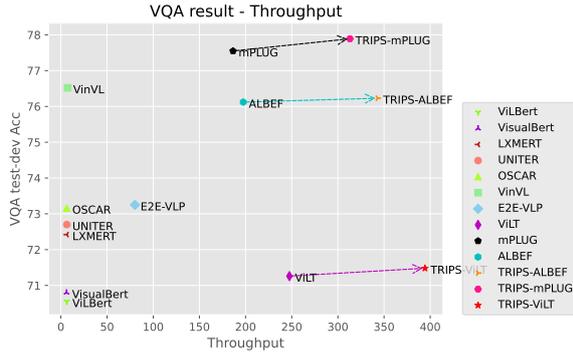


Fig. 4 The figure below visualizes the performance and inference speed distribution of different VLP models. The y-axis represents the accuracy of the VLP model on the test-dev dataset of VQA, while the x-axis represents the throughput of processing image-text pairs on a single 32G V100 GPU.

Table 7 The comparison of the efficiency of different models. FLOPs, throughput, and latency are reported here. Since FLOPs are proportional to input size, for a fair comparison, we use same the input size with (Kim et al, 2021), which is 197 for image patches length and 40 for text tokens length. We also keep the same setting when calculating throughput and latency.

Models	Latency	FLOPs	Throughput
ViLBERT	880ms	958.10	6.40
VisualBERT	910ms	425.20	6.10
LXMERT	980ms	952.20	6.38
UNITER _{Base}	870ms	949.90	6.42
OSCAR _{Base}	860ms	956.40	6.35
VinVL _{Base}	640ms	1023.30	7.32
E2E-VLP	70ms	144.30	80.23
ViLT _{Base}	15ms	55.40	247.53
TRIPS-ViLT	8ms	32.38	394.32
ALBEF _{Base}	22ms	33.42	197.52
TRIPS-ALBEF	11ms	20.89	343.05
mPLUG _{Base}	24ms	36.63	186.42
TRIPS-mPLUG	13ms	25.04	313.71

5.2 Efficiency of TRIPS

To investigate the efficiency of Text-Relevant Image Patch Selection, we first compare the computational complexity of various models. We report the Floating Point Operations Per Second (FLOPs), a widely used evaluation metric for model computational complexity. In addition, we evaluate the computational speed of our model by comparing the throughput and latency of different models. We use a Xeon Platinum 8163 CPU and

an NVIDIA V100 GPU to calculate the latency and throughput. As shown in Table 7, TRIPS not only exhibits the lowest computational complexity but also achieves the fastest computational speed (e.g., 343.05 throughput and 11ms latency for TRIPS-ALBEF vs. 197.52 throughput and 22ms latency for ALBEF).

To provide a more intuitive illustration of how TRIPS balances model efficiency and effectiveness, we visualize the performance and inference speed distribution of different VLP models on the VQA task in Figure 4. The figure clearly demonstrates that incorporating TRIPS consistently results in a speedup while maintaining competitive or superior performance across various VLP base models.

Similar to this visualization, the following further analyses will mainly be based on the VQA task to make the tables and figures more reader-friendly. Note that most conclusions apply to other tasks.

5.3 The Impact of Patch-section Location and Keep Rate

To assess the impact of patch-selection layer location and keep rate on the model’s efficiency and effectiveness, we train TRIPS-ALBEF with varying patch-selection locations and numbers of selected tokens, and test the yielding models on the VQA task. The results presented in Table 8 reveal two key observations.

First, positioning the patch-selection layer in shallower layers reduces computational complexity but negatively affects accuracy. For instance, when the patch-selection layer is placed before the third layer (i.e., at the second layer), accuracy significantly drops despite a notable increase in throughput. A possible explanation for this is that the attention maps between the text [CLS] embedding and the input tokens may be unreliable during the early processing of input tokens in shallow layers.

Second, fusing too many image tokens in the patch-selection layer can lead to a considerable decline in downstream task performance. For example, if we designate the 2nd and 4th layers in ViT as patch-selection layers and set the keep rate to 50%, performance on the VQA task decreases to 74.21, compared to 76.12 for the model without a patch-selection layer.

Table 8 Results of pre-training and finetuning TRIPS-ALBEF with different locations and keep rates. we report the text-dev score results of VQA, FLOPs and Throughput. In this table, we set the input image size to 384×384 and the length of input text is 40. The throughput (image-text/s) is measured on an NVIDIA V100 GPU using the largest possible batch size for our model.

Locations	Keep rates	Overall Keep rate	VQA test-dev	FLOPs (G)	Throughput
-	-	100%	76.12	76.03	79.32
[2]	50%	50%	75.60	42.17	161.26
[10]	50%	50%	76.19	63.84	96.66
[2,4]	50%	%25	74.21	28.00	238.41
[4,8]	50%	%25	74.93	38.82	165.30
[5,10]	50%	%25	75.29	44.22	143.37
[6,12]	50%	%25	75.48	49.63	126.46
[2,4]	70%	%49	74.87	43.96	153.92
[4,8]	70%	%49	75.94	51.72	125.55
[5,10]	70%	%49	76.23	55.60	115.01
[6,12]	70%	%49	76.24	59.48	106.07
[2,6,10]	70%	%34	74.92	42.66	156.13
[3,6,9]	70%	%34	75.09	43.49	151.40
[4,8,12]	70%	%34	75.23	49.74	129.81

Table 9 Results of TRIPS-ALBEF finetuning on VQA and NLVR task with different resolution images. When calculating FLOPs, the input length of the text is kept at 40 and the settings for calculating throughput are the same as Table 8.

Selection Layer	Keep rate	image size	VQA test-dev	FLOPs(G)	Troughout
-	-	384×384	76.12	76.03	79.32
[5,10]	70%	224×224	75.23	20.89	343.05
[5,10]	70%	256×256	75.84	26.61	258.03
[5,10]	70%	304×304	76.13	36.62	189.07
[5,10]	70%	384×384	76.23	55.60	115.01
[5,10]	70%	464×464	76.54	74.83	81.0
[5,10]	70%	512×512	76.83	84.13	72.10

5.4 Fine-tuning on Higher Resolution Images

We can manipulate the computational cost by fusing varying numbers of inattentive tokens. To demonstrate this, we fine-tune TRIPS-ALBEF, TRIPS-ViLT, and TRIPS-mPLUG on the VQA task, which uses images with different resolutions as input. The results are presented in Table 9 and Figure 5. These experimental findings indicate that by increasing the input image resolution, we can enhance the model’s performance by incorporating more image tokens. For instance, by fine-tuning TRIPS-ALBEF with images of size 464×464 , we can achieve a score of 76.54 on VQA, surpassing the baseline fine-tuned with images of 384×384 while maintaining a similar computational complexity.

5.5 Ablation Study

We also conduct ablation studies to investigate the effects of inattentive image token fusion and Text-aware Dynamic Attention (TD-ATT). In Table 5.4, *w/o* ITF denotes that the inattentive tokens are directly discarded without fusion. As demonstrated in Table 5.4, fusing inattentive tokens leads to better performance compared to the model without inattentive tokens. Although the improvement is modest, no additional computational overhead is introduced. We further examine the impact of Text-aware Dynamic Attention. Specifically, *w/o* TD-ATT indicates that we remove the TD-ATT from the patch-selection layer and select the image tokens based on the image [CLS] token. As TRIPS-ViLT is a single-stream model and the [CLS] token aggregates both

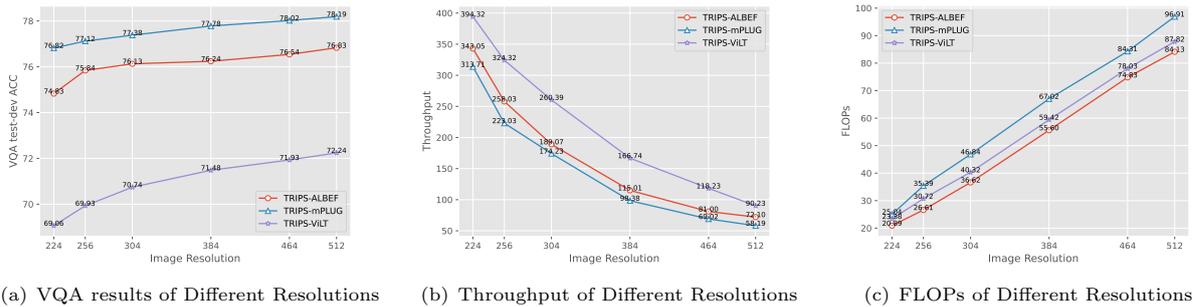


Fig. 5 Sub-figure (a) visualizes the VQA results of three models (TRIPS-ViLT, TRIPS-ALBEF, TRIPS-mPLUG) at different image resolutions, sub-figure (b) visualizes the throughput of three different models at different image resolutions, and sub-figure (c) visualizes the FLOPs of the three models at different image resolutions.

Table 10 The result of ablations. We finetune TRIPS-ViLT, TRIPS-ALBEF, and TRIPS-mPLUG on VQA and report test-dev results. The setting for calculating FLOPs and throughput is the same as Table 8. The same with the settings of TRIPS we present in the main results, we select the 5th and 10th as the patch selection layer, and each layer will keep 70% image tokens.

model	VQA	FLOPs(G)	Throughput
ALBEF-TRIPS	76.23	55.60	115.01
-w/o ITF	75.92	55.14	118.04
-w/o TD-ATT	75.23	53.44	120.23
ALBEF-mPLUG	77.89	67.02	98.38
-w/o ITF	77.29	65.23	103.38
-w/o TD-ATT	76.89	63.34	109.38
ALBEF-ViLT	71.48	59.42	166.74
-w/o ITF	70.63	57.19	172.01

image and text information, we cannot perform this ablation for it. As demonstrated in Table 5.4, selecting image patch tokens with the image [CLS] token without considering the linguistic context leads to a decline in the model’s performance. This result supports our initial motivation that directly removing patch tokens based on the image [CLS] without incorporating text knowledge is unsuitable for VLP models.

5.6 Visualization

The proposed TRIPS accelerates VLP through a novel patch selection module that identifies text-consistent image tokens in the vision backbone and preserves the attentive image tokens. To further investigate our model’s interpretability, we visualize the process of text-relevant image patch selection during both the pre-training and inference stages.



Fig. 6 The visualization of the selected text-aware image patches in different selection layers of TRIPS-mPLUG. We set the 5th and 10th layers in the vision backbone as the patch-selection layer, and we keep 70% image patches in each layer.

Figure 6 displays the selected text-relevant image patches during the pre-training stage. It is evident that as the network goes deeper, the inattentive tokens are gradually removed or fused,

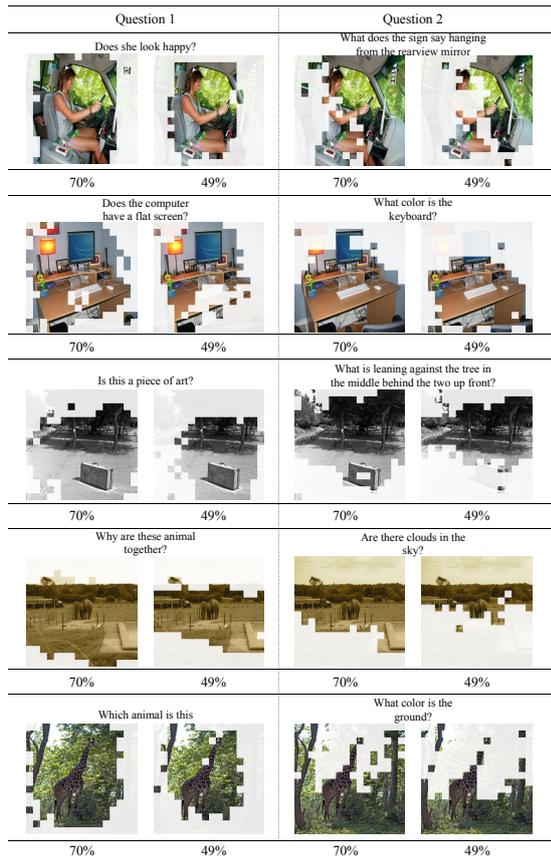


Fig. 7 The visualization of the selected text-aware image patches in different selection layers of TRIPS-mPLUG, conditioned on different text queries in the VQA scenario. We set the 5th and 10th layers in the vision backbone as the patch-selection layer, and we keep 70% image patches in each layer.

while the text-relevant tokens are selected and preserved.

Figure 7 visualizes the selected text-aware image patches in the VQA scenario to demonstrate the effectiveness of the text-relevant image patch selection module during the downstream task inference stage. We input various queries and visualize the text-aware image patches chosen by the text-relevant image patch selection module. As depicted in Figure 7, the selected image patches are highly relevant to the query texts, enabling our model to make accurate predictions.

6 Conclusion

We have presented TRIPS, an efficient VLP model with **Text-Relevant Image Patch Selection**, which

progressively eliminates redundant image tokens with the guidance of text. TRIPS incorporates a novel patch selection module within the vision backbone to select text-consistent image tokens. This module preserves attentive image tokens with text guidance and combines inattentive tokens into a single token by dynamically computing text-dependent visual attention in an end-to-end manner. Experiments demonstrate that our method not only reduces the computational cost of VLP but also enhances the efficiency of cross-modal fusion due to the decreased visual sequences, while maintaining or even improving the performance of downstream image-text tasks.

References

- Agrawal A, Lu J, Antol S, et al (2015) Vqa: Visual question answering. *International Journal of Computer Vision* 123:4–31
- Agrawal H, Desai K, Wang Y, et al (2018) nocaps: novel object captioning at scale. *CoRR* abs/1812.08658. URL <http://arxiv.org/abs/1812.08658>, 1812.08658
- Bi B, Li C, Wu C, et al (2020) Palm: Pre-training an autoencoding&autoregressive language model for context-conditioned generation. *arXiv preprint arXiv:200407159*
- Caron M, Touvron H, Misra I, et al (2021) Emerging properties in self-supervised vision transformers. *2021 IEEE/CVF International Conference on Computer Vision (ICCV)* pp 9630–9640
- Chen YC, Li L, Yu L, et al (2019) Uniter: Learning universal image-text representations. *ArXiv* abs/1909.11740
- Chen YC, Li L, Yu L, et al (2020) Uniter: Universal image-text representation learning. In: *ECCV*
- Choromanski K, Likhoshesterov V, Dohan D, et al (2021) Rethinking attention with performers. *ArXiv* abs/2009.14794
- Cubuk ED, Zoph B, Shlens J, et al (2020) Randaugment: Practical automated data augmentation with a reduced search space. In: *Proceedings of the IEEE/CVF Conference on Computer*

- Vision and Pattern Recognition Workshops, pp 702–703
- Devlin J, Chang MW, Lee K, et al (2019) Bert: Pre-training of deep bidirectional transformers for language understanding. ArXiv abs/1810.04805
- Dosovitskiy A, Beyer L, Kolesnikov A, et al (2021) An image is worth 16x16 words: Transformers for image recognition at scale. ArXiv abs/2010.11929
- Dou ZY, Xu Y, Gan Z, et al (2021) An empirical study of training end-to-end vision-and-language transformers. arXiv preprint arXiv:211102387
- Fang Z, Wang J, Hu X, et al (2021) Compressing visual-linguistic model via knowledge distillation. In: Proceedings of the IEEE/CVF International Conference on Computer Vision, pp 1428–1438
- Gan Z, Chen YC, Li L, et al (2021) Playing lottery tickets with vision and language. In: AAAI Conference on Artificial Intelligence
- Goyal Y, Khot T, Summers-Stay D, et al (2017) Making the v in vqa matter: Elevating the role of image understanding in visual question answering. In: Proceedings of the IEEE conference on computer vision and pattern recognition, pp 6904–6913
- He K, Gkioxari G, Dollár P, et al (2017) Mask r-cnn. 2017 IEEE International Conference on Computer Vision (ICCV) pp 2980–2988
- Heo B, Yun S, Han D, et al (2021) Rethinking spatial dimensions of vision transformers. 2021 IEEE/CVF International Conference on Computer Vision (ICCV) pp 11916–11925
- Huang Z, Zeng Z, Liu B, et al (2020) Pixel-bert: Aligning image pixels with text by deep multi-modal transformers. ArXiv abs/2004.00849
- Jia C, Yang Y, Xia Y, et al (2021) Scaling up visual and vision-language representation learning with noisy text supervision. arXiv preprint arXiv:210205918
- Karpathy A, Fei-Fei L (2015) Deep visual-semantic alignments for generating image descriptions. In: Proceedings of the IEEE conference on computer vision and pattern recognition, pp 3128–3137
- Kim W, Son B, Kim I (2021) Vilt: Vision-and-language transformer without convolution or region supervision. In: ICML
- Kitaev N, Kaiser L, Levskaya A (2020) Reformer: The efficient transformer. ArXiv abs/2001.04451
- Krishna R, Zhu Y, Groth O, et al (2016) Visual genome: Connecting language and vision using crowdsourced dense image annotations. International Journal of Computer Vision 123:32–73
- Li C, Xu H, Tian J, et al (2022a) mplug: Effective and efficient vision-language learning by cross-modal skip-connections
- Li J, Selvaraju RR, Gotmare AD, et al (2021) Align before fuse: Vision and language representation learning with momentum distillation. In: NeurIPS
- Li J, Li D, Xiong C, et al (2022b) Blip: Bootstrapping language-image pre-training for unified vision-language understanding and generation. arXiv preprint arXiv:220112086
- Li LH, Yatskar M, Yin D, et al (2019) Visualbert: A simple and performant baseline for vision and language. ArXiv abs/1908.03557
- Li X, Yin X, Li C, et al (2020) Oscar: Object-semantic aligned pre-training for vision-language tasks. In: ECCV
- Liang Y, Ge C, Tong Z, et al (2022) Not all patches are what you need: Expediting vision transformers via token reorganizations. ArXiv abs/2202.07800
- Lin TY, Maire M, Belongie SJ, et al (2014) Microsoft coco: Common objects in context. In: ECCV
- Liu Z, Lin Y, Cao Y, et al (2021) Swin transformer: Hierarchical vision transformer using

- shifted windows. 2021 IEEE/CVF International Conference on Computer Vision (ICCV) pp 9992–10002
- Loshchilov I, Hutter F (2019) Decoupled weight decay regularization. In: ICLR
- Lu J, Batra D, Parikh D, et al (2019) Vilbert: Pretraining task-agnostic visiolinguistic representations for vision-and-language tasks. In: NeurIPS
- Ordonez V, Kulkarni G, Berg TL (2011) Im2text: Describing images using 1 million captioned photographs. In: NIPS
- Plummer BA, Wang L, Cervantes CM, et al (2015) Flickr30k entities: Collecting region-to-phrase correspondences for richer image-to-sentence models. *International Journal of Computer Vision* 123:74–93
- Radford A, Kim JW, Hallacy C, et al (2021) Learning transferable visual models from natural language supervision. In: ICML
- Rao Y, Zhao W, Liu B, et al (2021) Dynamicvit: Efficient vision transformers with dynamic token sparsification. In: *Neural Information Processing Systems*
- Redmon J, Divvala SK, Girshick RB, et al (2016) You only look once: Unified, real-time object detection. 2016 IEEE Conference on Computer Vision and Pattern Recognition (CVPR) pp 779–788
- Ren S, He K, Girshick RB, et al (2015) Faster r-cnn: Towards real-time object detection with region proposal networks. *IEEE Transactions on Pattern Analysis and Machine Intelligence* 39:1137–1149
- Rennie SJ, Marcheret E, Mroueh Y, et al (2017) Self-critical sequence training for image captioning. In: 2017 IEEE Conference on Computer Vision and Pattern Recognition (CVPR), pp 1179–1195, <https://doi.org/10.1109/CVPR.2017.131>
- Ryoo MS, Piergiovanni AJ, Arnab A, et al (2021) Tokenlearner: Adaptive space-time tokenization for videos. In: NeurIPS
- Sharma P, Ding N, Goodman S, et al (2018) Conceptual captions: A cleaned, hypernymed, image alt-text dataset for automatic image captioning. In: ACL
- Singh A, Hu R, Goswami V, et al (2021) Flava: A foundational language and vision alignment model. ArXiv abs/2112.04482
- Su W, Zhu X, Cao Y, et al (2020) Vi-bert: Pre-training of generic visual-linguistic representations. ArXiv abs/1908.08530
- Suhr A, Zhou S, Zhang I, et al (2019) A corpus for reasoning about natural language grounded in photographs. ArXiv abs/1811.00491
- Tan HH, Bansal M (2019) Lxmert: Learning cross-modality encoder representations from transformers. ArXiv abs/1908.07490
- Touvron H, Cord M, Douze M, et al (2021) Training data-efficient image transformers & distillation through attention. In: ICML
- Vaswani A, Shazeer NM, Parmar N, et al (2017) Attention is all you need. ArXiv abs/1706.03762
- Wang J, Hu X, Zhang P, et al (2020a) Minivlm: A smaller and faster vision-language model. arXiv preprint arXiv:201206946
- Wang S, Li BZ, Khabsa M, et al (2020b) Linformer: Self-attention with linear complexity. ArXiv abs/2006.04768
- Wang W, Bao H, Dong L, et al (2021a) Vlmo: Unified vision-language pre-training with mixture-of-modality-experts. ArXiv abs/2111.02358
- Wang W, Xie E, Li X, et al (2021b) Pyramid vision transformer: A versatile backbone for dense prediction without convolutions. 2021 IEEE/CVF International Conference on Computer Vision (ICCV) pp 548–558
- Wang Z, Yu J, Yu AW, et al (2021c) Simvlm: Simple visual language model pretraining with weak supervision. ArXiv abs/2108.10904

- Wu H, Xiao B, Codella NCF, et al (2021) Cvt: Introducing convolutions to vision transformers. 2021 IEEE/CVF International Conference on Computer Vision (ICCV) pp 22–31
- Xu H, Yan M, Li C, et al (2021a) E2e-vlp: End-to-end vision-language pre-training enhanced by visual learning. ArXiv abs/2106.01804
- Xu Y, Zhang Z, Zhang M, et al (2021b) Evo-vit: Slow-fast token evolution for dynamic vision transformer. ArXiv abs/2108.01390
- Yang Z, Gan Z, Wang J, et al (2021) Crossing the format boundary of text and boxes: Towards unified vision-language modeling. CoRR abs/2111.12085. URL <https://arxiv.org/abs/2111.12085>, 2111.12085
- Yu F, Tang J, Yin W, et al (2021) Ernie-vil: Knowledge enhanced vision-language representations through scene graph. In: AAAI
- Yu L, Poirson P, Yang S, et al (2016) Modeling context in referring expressions. In: European Conference on Computer Vision, Springer, pp 69–85
- Zhang P, Li X, Hu X, et al (2021) Vinvl: Revisiting visual representations in vision-language models. 2021 IEEE/CVF Conference on Computer Vision and Pattern Recognition (CVPR) pp 5575–5584
- Zhou L, Palangi H, Zhang L, et al (2020) Unified vision-language pre-training for image captioning and vqa. ArXiv abs/1909.11059
- Zong Z, Li K, Song G, et al (2021) Self-slimmed vision transformer. ArXiv abs/2111.12624

Appendix A Comparison Models

- **E2E-VLP** (Xu et al, 2021a): proposes the first end-to-end VLP method for both V+L understanding and generation, with a unified Transformer encoder-decoder architecture.
- **VinVL** (Zhang et al, 2021): pre-trains a large-scale object-attribute detection model with much larger amounts of supervised data on four public object detection datasets for extracting better region-based visual features.
- **OSCAR** (Li et al, 2020): proposes to use object tags detected in images as anchor points to ease the learning of cross-modal alignments, where the input to the Transformer is a combination of image, text, and object tags.
- **METER** (Dou et al, 2021): systematically investigates how to design and pre-train a fully transformer-based VL model in an end-to-end manner.
- **VLMO** (Wang et al, 2021a): presents a unified vision-language pre-trained model that jointly learns a dual encoder and a fusion encoder with a modular Transformer network.
- **SimVLM** (Wang et al, 2021c): different from previous VLP methods that only use limited (4M-10M) image-text pairs for pre-training, it proposes a simple VLP model with a single prefix language modeling objective, which pre-trains on an extremely large aligned cross-modal data of about 1.8B noisy image-text pairs. This is also the latest state-of-the-art method of image captioning.
- **ALBEF** (Li et al, 2021): introduces a contrastive loss to align the image and text representations before fusing them through cross-modal attention, which enables more grounded vision and language representation learning.
- **UNITER** (Chen et al, 2020): proposes an improved single-stream VLP method, by designing two new pre-training strategies: 1) it uses conditional masking on pre-training tasks instead of random masking strategy, 2) it designs a new word-region alignment pre-training task via the use of optimal transport to explicitly encourage fine-grained alignment between words and image regions.
- **ALIGN** (Jia et al, 2021): leverages a noisy dataset of over one billion image alt-text pairs,

obtained without expensive filtering or post-processing steps in the Conceptual Captions dataset.

- **ViLT** (Kim et al, 2021): adopts linear projection and word embedding as the visual and textual encoders, and uses the visual transformer as the cross-modal encoder to align and fuse the features of both modalities in an end-to-end manner.
- **BLIP** (Li et al, 2022b): proposes a new VLP framework that transfers flexibly to both vision-language understanding and generation tasks. It effectively utilizes noisy web data by bootstrapping the captions.
- **UNICORN** (Yang et al, 2021): proposes a vision-language (VL) model that unifies text generation and bounding box prediction into a single architecture.
- **LXMERT** (Tan and Bansal, 2019): is the pioneering work to pre-train a dual-stream multi-modal Transformer, which consists of an object relationship encoder, a language encoder, and a cross-modality encoder. It is widely used as a baseline method for VLP models.
- **ViLBERT** (Lu et al, 2019): proposes the first work that extends the BERT architecture to a multi-modal dual-stream VLP model, which processes both visual and textual inputs in separate streams that interact through co-attentional transformer layers.
- **mPLUG** (Li et al, 2022a): is a vision-language foundation model for both cross-modal understanding and generation and introduces an effective and efficient vision-language architecture with novel cross-modal skip-connections.

Appendix B Downstream Task Details

We evaluate TRIPS on the four downstream vision-language tasks. The hyperparameters that we use for finetuning on the downstream tasks are listed in Table B1. Following (Li et al, 2021), all tasks adopt RandAugment, AdamW optimizer with a weight decay of 0.05 and a cosine learning rate schedule. Next, we introduce the dataset settings in detail.

Table B1 Finetuning hyperparameters for downstream tasks. † denotes two stages of fine-tuning.

Task	LR (ViT-L/BERT _{base})	batch size	epochs
VQA	2e-5/5e-6	1024	8
Captioning†	1e-5&8e-7	256	5
Retrieval	1e-5/2e-6	256	5
NLVR2	5e-5/5e-6	256	15
Visual Grounding	2e-5/2e-6	512	120

VQA.

The VQA task (Agrawal et al, 2015) requires the model to answer natural language questions given an image. Most methods (Tan and Bansal, 2019; Wang et al, 2021a; Li et al, 2020; Wang et al, 2021c) deal with visual question answering tasks as multi-label classification on pre-defined answer sets. This strategy achieves strong performance, but it is not suitable for real-world open scenarios. We conduct an experiment on the VQA2.0 dataset (Goyal et al, 2017), which contains 83k/41k/81k images for training/validation/test. Following (Li et al, 2021), we use both training and validation splits for training, and incorporate additional training data from Visual Genome (Krishna et al, 2016). Following (Li et al, 2020), we concatenate the question with the object labels and OCR tokens extracted from the image.

Image Captioning.

Image captioning requires generating a descriptive and fluent caption for a given image. We evaluate the performance of TRIPS on two popular datasets: COCO Caption (Lin et al, 2014) and NoCaps (Agrawal et al, 2018). We fine-tune TRIPS-mPLUG on the training set of COCO Caption and test it on the same Karpathy split (Li et al, 2020; Wang et al, 2021c) as well as the NoCaps validation set. To fine-tune TRIPS-mPLUG on COCO Caption, we follow the approach in (Li et al, 2020) and first train the model with the cross-entropy loss for 5 epochs with a learning rate of 1e-5 and a batch size of 256. We then further fine-tune the model with CIDEr optimization (Rennie et al, 2017) for an additional 5 epochs with a smaller learning rate of 8e-7. We use the best checkpoint on COCO Caption to predict on the NoCaps validation set. During inference, we use beam search with a beam size of 10 and set the maximum generation length to 20.

Image-Text Retrieval.

We conducted experiments on both image-to-text retrieval (TR) and text-to-image retrieval (IR) using the COCO (Lin et al, 2014) and Flickr30K (Plummer et al, 2015) datasets and used the widely-used Karpathy split (Karpathy and Fei-Fei, 2015) for both. COCO contains 113k/5k/5k images for train/validation/test, while Flickr30K contains 29k/1k/1k images for train/validation/test. During fine-tuning, for TRIPS-ALBEF and TRIPS-mPLUG we jointly optimized the ITC loss and the ITM loss following the approach in (Li et al, 2021, 2022b). During inference, we first selected the top-k candidates by computing the dot-product similarity between the image and text encoder features (We set $k = 256$ for COCO and $k = 128$ for Flickr30K). For the efficiency of coarse-grained ranking, we directly selected the patch based on the attention weights of the image [CLS] token to other patch tokens.

Visual Grounding.

The task of visual grounding involves localizing the referred object in an image given a plain text query. Instead of directly regressing bounding boxes, our approach concatenates visual features with textual features, which are then fed into the multi-modal decoder to predict the object’s coordinates. We evaluate our method on the referring expression grounding dataset: RefCOCO+ (Yu et al, 2016). The RefCOCO+ dataset contains 19K images and 141K queries.

NLVR2.

The NLVR2 (Suhr et al, 2019) task requires the model to predict whether a sentence. We conduct experiments following the original train/val/test split in (Suhr et al, 2019). Following (Li et al, 2022b), we use two cross-attention layers to process the two input images, and their outputs are merged and fed to the FFN. An MLP classifier is then applied to the output embedding of the language [CLS] token.